Pergamon

Journal of Structural Geology, Vol. 18, No. 8, pp. 1079 to 1087, 1996

0191–8141/96 $15.00 + 0.00

PII: S0191–8141(96)00024–7

Refolding by flexural flow

S. K. GHOSH

Department of Geological Sciences, Jadavpur University, Calcutta 700 032, India

(*Received* 5 *September* 1995; *accepted in revised form* 11 *March* 1996)

Abstract—The existing method of derivation of the magnitude of simple shear (γ) in flexural slip and flexural flow folds has been extended to the general case of folds in which the radius of curvature varies continuously over a fold arc of any shape. In agreement with earlier conclusions, the present analysis shows that γ is equal to the dip angle (θ) measured in radians. This result is applied to the situation in which an early fold (F_1) on a passively behaving layer is refolded by flexural flow on the axial planar cleavage of F_1. Both the theory and the folding experiments with paper stacks show that the F_2 folds on the passively behaving layers show an unusual pattern of thickness variation, with the orthogonal thickness continuously increasing or continuously decreasing from one limb to the other without a maximum or a minimum at the hinge. Flexural slip or flexural flow folds may be identified from this characteristic pattern of thickness variation. The asymmetry of the smaller F_1 folds on the layering is strongly modified by later folding on the axial planar cleavage.

INTRODUCTION

The refolding of an earlier generation of folds by a later generation of shear folds has been analysed by O'Driscoll (1962), Ramsay (1967), Thiessen & Means (1980) and Thiessen (1986). Similarly, the development of a refold structure by superposed buckling has been described by several authors, e.g. Ghosh & Ramberg (1968), Skjernaa (1975), Ghosh *et al.* (1992, 1993). The present paper is concerned with the modification of the fold shape and layer-thickness when an earlier generation of folds (say, F_1) is refolded by flexural flow or flexural slip. In the model of shear folding, the layer behaves in a passive manner and the folding occurs in response to heterogeneous simple shear at an angle to the layering. In the present model of refolding by flexural flow, the stack of slip surfaces is deformed to parallel folds but the magnitude of simple shear displacement varies along a single surface. At each point of this folded surface the layer-segment is externally rotated but the angle between it and the intersecting slip surfaces changes entirely in response to the simple shear displacement parallel to the slip surfaces.

The distinction between flexural slip and flexural flow folds depends on the scale of observation. In practice, the structure can be regarded as a flexural flow fold if the surfaces along which the simple shear movement takes place are very closely spaced so that a marker line oblique to these surfaces appears as a more or less continuous line after its deformation. Folding of penetrative cleavage surfaces may give rise to flexural flow folds. If there is a passively behaving colour banding, such as bedding in slates, oblique to the cleavage, its orthogonal thickness will vary in accordance with the magnitude and sense of simple shear. The resulting fold geometry may be quite complex. In the following discussion the surfaces along which flexural slip or flexural flow takes place will be designated S_c and the bounding surfaces of the passive layers will be designated S_b.

MAGNITUDE OF SIMPLE SHEAR IN FLEXURAL FLOW

For any analysis of flexural flow or flexural slip folds it is essential to know the magnitude of simple shear at any point within the fold. At first glance it may seem difficult to obtain this crucial information. Fortunately, as shown by Ramsay (1967, p. 393; see also Ramsay & Huber, 1987, p. 456, fig. 21.4), this information is readily available from the fold shape alone.

Flexural slip and flexural flow folds have been discussed in detail by Ramsay (1967) and by Ramsay & Huber (1987). Ramsay considered a folded surface made up of a number of discrete circular arcs of radii r_1, r_2 etc., which make angles δ_1, δ_2 etc. at their respective centres. He showed that at any point, say at the end of the third consecutive arc from the hinge point, the simple shear strain (γ) will be a sum of these angles ($\delta_1 + \delta_2 + \delta_3$) measured in radians. This unexpectedly simple result can be utilized to determine the strain at any point in a flexural flow fold. The result is of such importance that it is worthwhile to check whether the same solution can be derived for a fold-arc without a discontinuity in the dip angle and with continuous variation of the curvature.

The following derivation is valid for folds of any shape. Only a quarter wave of a fold is considered in which the dip angle θ is zero at the hinge point and increases continuously away from it. Let us consider two parallel fold arcs C_1 and C_2 at a constant distance t from each

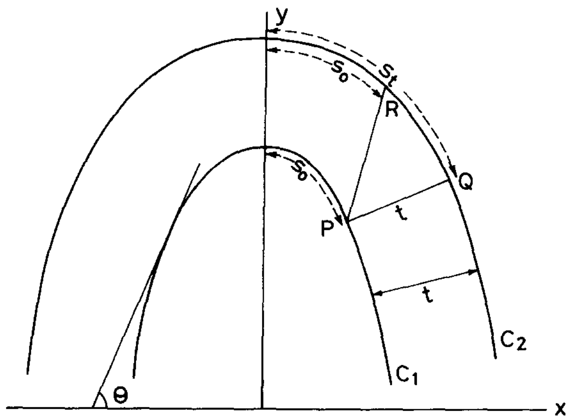

Fig. 1. Simple shear displacement parallel to slip surfaces of a flexural slip fold. C_1 and C_2 are two fold arcs at a distance t from each other. P is a current point on C_1. PQ is normal to C_1 and C_2. The arc-length distance of P from the hinge point is s_0 and the arc-length distance of Q from the hinge point of C_2 is s_t. R is a point on C_2 such that its arc-length distance from the hinge point of C_2 is s_0. Hence RQ is the magnitude of slip on C_2.

other. Let the lower curve C_1 (Fig. 1) be represented by the function $y = a(x)$ and the upper curve C_2 be represented by the function $y = b(x)$. For each of these curves the arc-length s measured from the hinge point is a function of x and the dip angle θ is also a function of x. Hence, for each of these curves s is a function of θ, say,

$$s = f(\theta) \text{ for } C_1,$$

$$s = g(\theta) \text{ for } C_2. \tag{1}$$

Since the curves C_1 and C_2 will not have any straight line portion in them, the correspondence between s and θ will be one to one for both of them and therefore, for both C_1 and C_2, θ is also a function of s. Let

$$\theta = \varphi(s) \text{ for } C_1,$$

$$\theta = \psi(s) \text{ for } C_2. \tag{2}$$

For any dip angle θ, the curvature at any point P on C_1 (Fig. 1) is $\varphi'(s) = \frac{\mathrm{d}}{\mathrm{d}s}\varphi(s)$ and the curvature at the corresponding point Q on C_2 is $\psi'(s) = \frac{\mathrm{d}}{\mathrm{d}s}\psi(s)$, PQ being a normal to both C_1 and C_2:

$$\varphi'(s) = \frac{1}{r},$$

$$\psi'(s) = \frac{1}{r+t}, \tag{3}$$

where t is the orthogonal thickness and r is the radius of curvature of C_1 at P. By a well-known theorem of derivatives, we have

$$\varphi'(s) = \frac{1}{f'(\theta)},$$

$$\psi'(s) = \frac{1}{g'(\theta)}, \tag{4}$$

where $f'(\theta) = \frac{\mathrm{d}}{\mathrm{d}\theta}f(\theta)$ and $g'(\theta) = \frac{\mathrm{d}}{\mathrm{d}\theta}g(\theta)$, so that

$$f'(\theta) = r,$$

$$g'(\theta) = r + t \tag{5}$$

and

$$g'(\theta) - f'(\theta) = t. \tag{6}$$

After integration we find

$$g(\theta) - f(\theta) = t\theta, \tag{7}$$

noting that at the hinge point $\theta = 0$, the amount of flexural slip, $g(\theta) - f(\theta) = 0$, or,

$$\frac{s_t - s_0}{t} = \theta \tag{8}$$

where s_t and s_0 are the arc-lengths of C_2 and C_1 at Q and P respectively.

But

$$\lim_{t\to 0}\frac{s_t - s_0}{t} = \gamma.$$

Therefore,

$$\gamma = \theta, \tag{9}$$

in agreement with Ramsay's conclusion. Thus, the magnitude of simple shear is equal to the dip angle measured in radians. The result is of considerable importance because it allows determination of the strain at any point in a flexural flow fold. It also sets an upper limit of the magnitude of simple shear. Since most natural folds are not fan folds the dip angle at the point of inflection of a fold cannot exceed 90° and the maximum value of simple shear cannot be greater than $\frac{\pi}{2}$ or 1.57.

VARIATION OF ORTHOGONAL THICKNESS OF A LAYER OBLIQUE TO SURFACES OF FLEXURAL FLOW

In the following analysis it is assumed that flexural flow folding has taken place on a set of fine penetrative S surfaces S_c, say a cleavage. It is also assumed that there is no hinge migration during the folding of S_c. There was before the folding, a layer of initial thickness t^*. The layering S_b may be a bedding or colour banding. The initial angle between S_c and S_b is ϕ (Fig. 2a). After folding, the angle ϕ changes to ϕ' by simple shear parallel to S_c. Depending on the sense of simple shear, ϕ' may be smaller or larger than ϕ. In the flexural flow fold, the orientation of S_c at the hinge zone is taken as horizontal and the dip angle of S_c at any point is designated θ. The dip angle of the folded S_b is designated α. Then

$$\alpha = \theta + \phi' \tag{10}$$

(Fig. 2b). Since $\cot\phi' = \cot\phi + \gamma$, or by eqn (9),

$$\cot\phi' = \cot\phi + \theta, \tag{11}$$

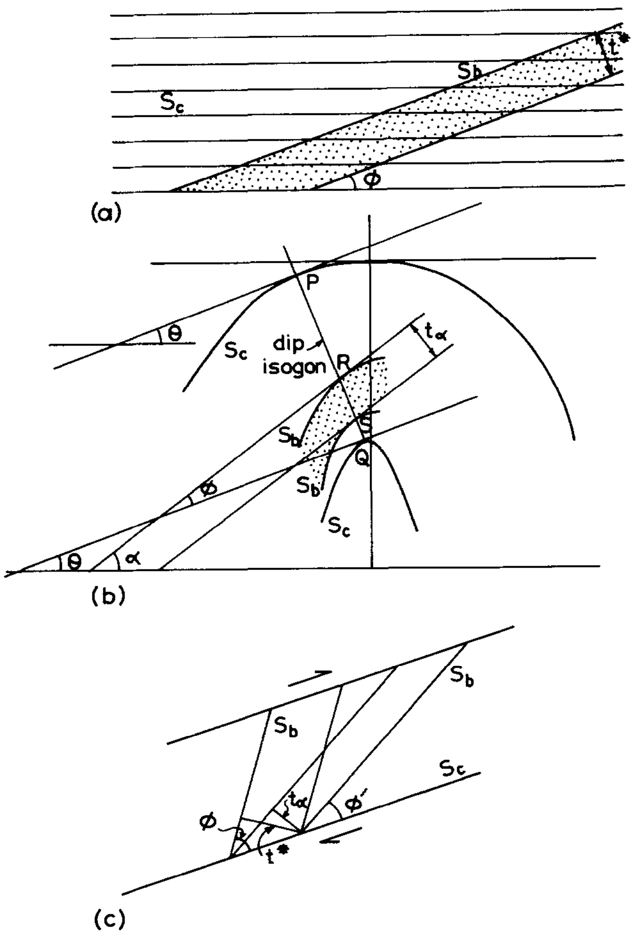

Fig. 2. (a) A layer S_b, with initial thickness t^*, at an angle ϕ to the slip surfaces S_c. (b) S_c forms a flexural flow fold. The tangent at its hinge point is horizontal. θ is the dip angle of S_c. The dip angle of S_b, with reference to the horizontal line, is α. The angle between the tangents to S_c and S_b at R is ϕ'. The dip isogons of S_c and S_b at P and R are coincident, although for different values of θ and α. The orthogonal thickness of the layer at R is t_α. (c) Simple shear displacement parallel to S_c rotates S_b so that its angle with S_c changes from ϕ to ϕ'. There is a corresponding change in the orthogonal thickness from t^* to t_α.

we can express the dip angle α of S_b at any point by the initial angle ϕ and the dip angle (θ) of S_c:

$$\alpha = \theta + \tan^{-1}\left(\frac{1}{\cot\phi + \theta}\right). \tag{12}$$

The sign convention for measuring α and θ is shown in Fig. 3.

Equation (12) shows that at the hinge point of the fold on S_c, i.e. at the point where $\theta = 0$, the dip angle α of the layering $\neq 0$. Since the simple shear vanishes at this hinge point, ϕ remains unchanged, and $\alpha = \phi$. At the hinge point of the fold on S_b, $\alpha = 0$. θ_h, the value of θ at this hinge point, as obtained from eqn. (12), is

$$\theta_h = -\tan^{-1}\left(\frac{1}{\cot\phi + \theta_h}\right) \tag{13}$$

or,

$$\theta_h + \cot\theta_h = -\cot\phi. \tag{14}$$

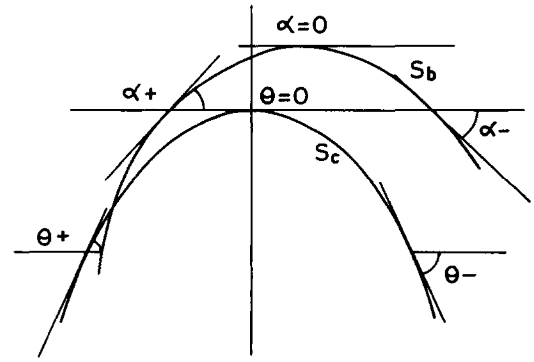

Fig. 3. Sign convention for θ and α.

Figure 4 shows the variation of θ_h with ϕ.

If t^* is the original thickness of the layer and t_α is the thickness of the layer after deformation, it is evident from Fig. 2(c) that,

$$\frac{t_\alpha}{t^*} = \frac{\sin\phi'}{\sin\phi}. \tag{15}$$

$$t'_\alpha = \frac{t_\alpha}{t^*} / \frac{t_0}{t^*} = \frac{t_\alpha}{t_0}, \tag{16}$$

where t_0 is the value of t_α for $\alpha = 0$.

To plot the t'_α/α curves for a particular value of ϕ, the following procedure can be adopted. For different values of θ, α is first calculated from eqn (12). For each of these

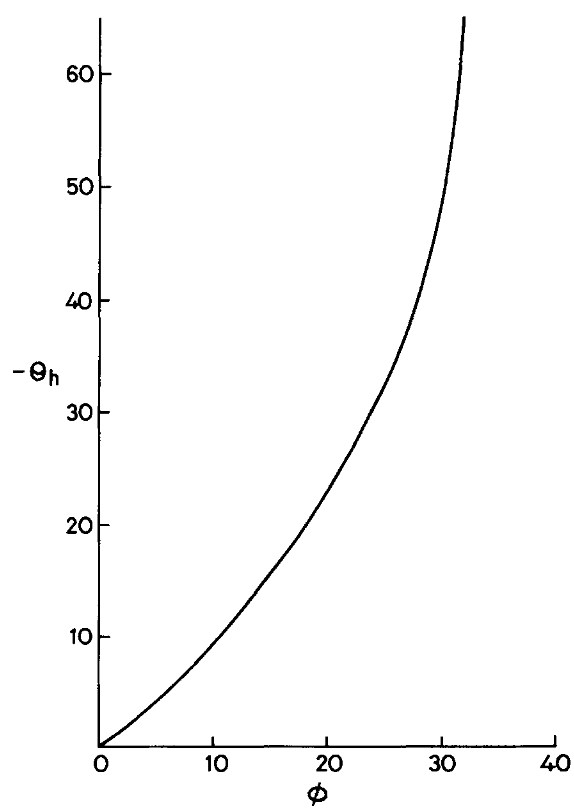

Fig. 4. Variation of θ_h with ϕ.

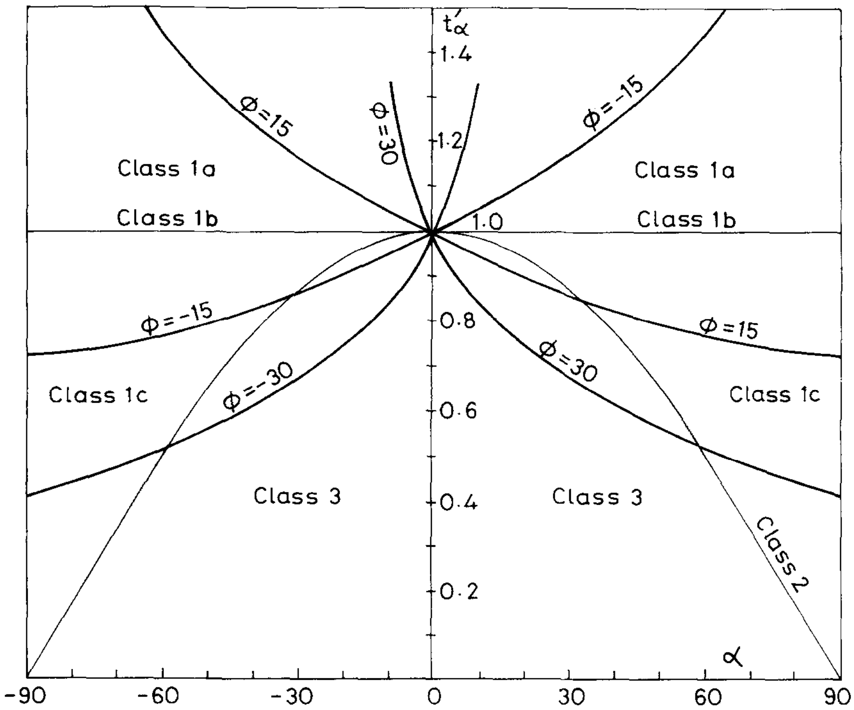

Fig. 5. t'_α/α plots for $\phi = \pm 15°$ and $\pm 30°$.

values of θ and the corresponding value of α, ϕ' is then determined from eqn (10) or (11). t_α/t^* can be calculated from eqn. (15). To determine t_0/t^*, θ_h is first determined from the graph of Fig. 4. t_0/t^* is then determined by following the same procedure as for t_α/t^*, but for $\alpha = 0$. Finally, t'_α is calculated from eqn (16).

Figure 5 shows the variation of t'_α with α for $\phi = \pm 15°$ and 30°. The figure shows that the geometry of the fold is quite different from any of the standard categories of fold classification. t'_α is neither a maximum nor a minimum at the fold hinge; it continuously increases or continuously decreases from one limb to the other across the fold hinge. This is the characteristic pattern of thickness variation for all such folds with any initial value of ϕ. The geometry of the folds can also be represented by plotting t_α/t^* against θ (Fig. 6). At the hinge of the fold on cleavage where $\theta = 0$, $\phi' = \phi$ and t_α is equal to the initial thickness (t^*) of the layer.

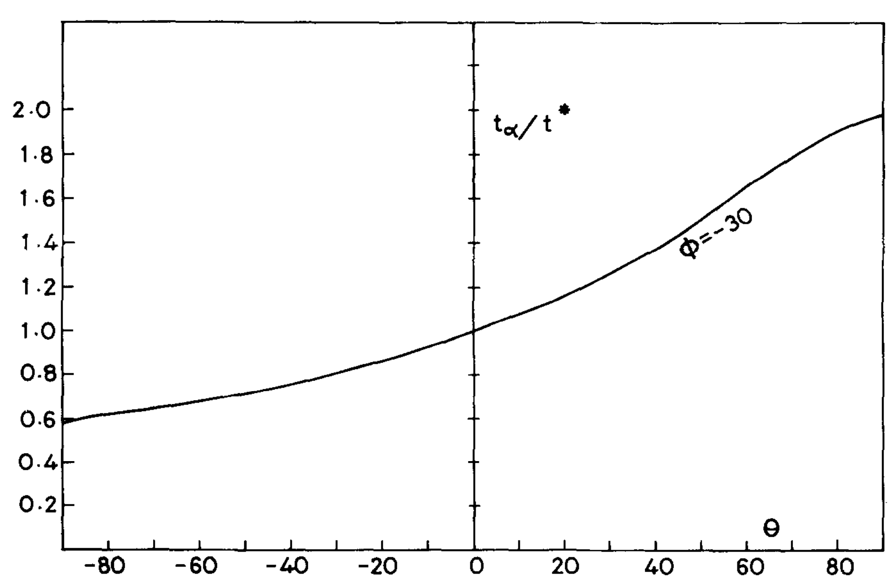

Fig. 6. Plot of t_α/t^* against θ for $\phi = -30°$. At the hinge point of the fold on S_c, i.e. at $\theta = 0$, the orthogonal thickness t_α is equal to the original thickness t^*.

The representation of the fold shape in transverse profile, by the variation of the orthogonal thickness with the dip angle (Ramsay 1967), depends on the choice of the line with respect to which the dip angle is measured. For simple folds the tangent at the hinge point is taken as the reference line. At this point the dip isogon is perpendicular to the tangent. The parallel flexural flow fold on S_c represents such a simple situation in which the reference line $\theta = 0$ can be chosen as the tangent to S_c at the hinge point. However, if we choose a line parallel to this line as the datum for measuring α for the fold of S_b, we find that the dip isogon of the layer at $\alpha = 0$ is not at a right angle to the tangent at this point (Fig. 7). For some folds, as suggested by Hudleston (1973), it is convenient to choose the reference line as the tangent to the folded surface at that point where the orthogonal thickness is a maximum and the dip isogon is normal to the folded surface. However, for the present case, this method is also inapplicable because the orthogonal thickness does not have a stationary value (either a maximum or a minimum) anywhere on the fold; the orthogonal thickness continuously increases from one limb to the other. Nevertheless, the shape of fold on the profile plane can be represented very well if, as suggested by Gray & Durney (1979), the variation of t' is shown by a continuous curve from one limb to the other (Fig. 5) and if the reference line tangential to S_b is parallel to a line $\theta = 0$.

Consider a line normal to S_c at any point of the fold. The dip angle θ of S_c is the same at all points of this line. Since, by eqn. (9), $\theta = \gamma$, the angle (ϕ') between S_b and S_c is also the same for each point along this line. Hence the dip isogon for S_b is coincident with the dip isogon for S_c, although for different values of θ and α. Thus, although the fold on S_b does not belong to any of the standard categories (1A, 1B, 1C, 2 or 3) its convergent pattern of dip isogons is identical to that of the parallel fold on S_c (Fig. 8).

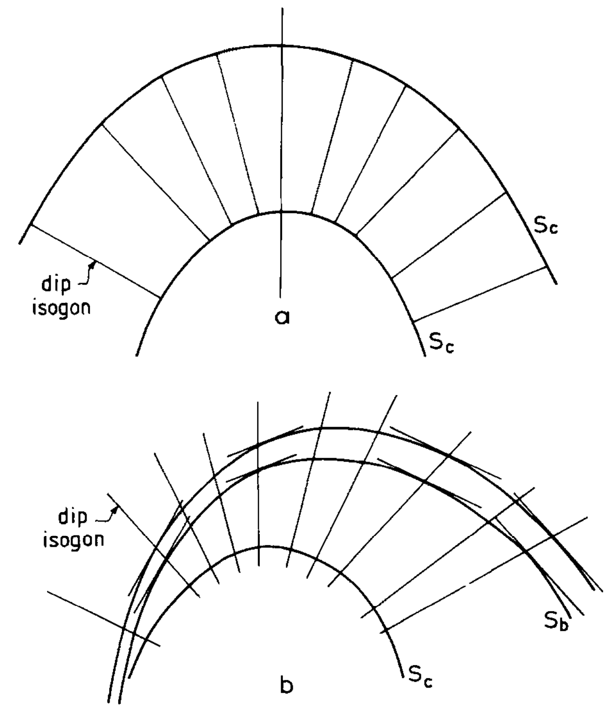

Fig. 8. Convergent dip isogons for (a) S_c and (b) S_b.

GEOMETRY OF SUPERPOSED FOLDS IN OBLIQUE LAYERS

Refolding by flexural flow is associated with the thickness-modification of passively behaving layers oblique to the slip surfaces. The modified fold shapes can be studied from paper stack models on the edge of which the first fold profile is drawn. In Fig. 9(a) the profile of a non-isoclinal straight limbed fold is drawn so that its axial trace is parallel to the traces of the paper sheets. The surfaces of the sheets act as slip surfaces S_c whereas the fold drawn on the edge represents the traces of S_b. Consider a non-isoclinal fold (F_1) with an axial planar S_c (Fig. 9a). The S_c surfaces are folded coaxially (F_2) by flexural flow (Figs. 9b & c and 10). Each of the two limbs, A and B (as in Fig. 11), of F_1 shows a continuous increase or a continuous decrease in orthogonal thickness from one limb of F_2 to the other. On one limb of F_2, the thickness of A increases whereas the thickness of B decreases from the limb to the hinge. The F_2 axial surface traces on A and B show a sideways shift (Ramsay 1967, p. 509) with respect to each other and the fold hinges lie on opposite sides of the axial trace of the F_2 fold on S_c (Fig. 11). The sense of shifting of the F_2 axial surface traces is the same as in superposed shear folds (Ramsay 1967, p. 509) as well as in the majority of superposed buckle folds (Ghosh 1995). In areas of superposed folding the noses of early folds (F_1) are often difficult to locate. The side-stepping of the axial surface traces of the later folds (F_2) in the outcrops enables us to locate the F_1 axial trace. From the sense of offset of the F_2 axial traces one can also determine on which side the F_1 fold closure is expected to lie (Ghosh, 1995). If F_2 is a flexural slip or a flexural flow fold on the axial plane cleavage of F_1 and if the limbs of F_1 have deformed in a passive manner, the axial surface trace of F_1 can also be located from the dissimilar patterns of thickness variation on any one limb of F_2 on either side of a line along which the F_1 axial trace should lie (Fig. 12).

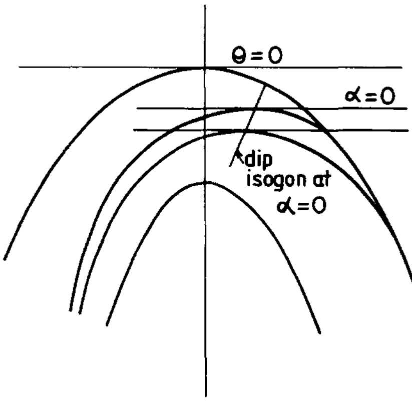

Fig. 7. At $\alpha = 0$, the dip isogon is not at a right angle to the tangent to S_b.

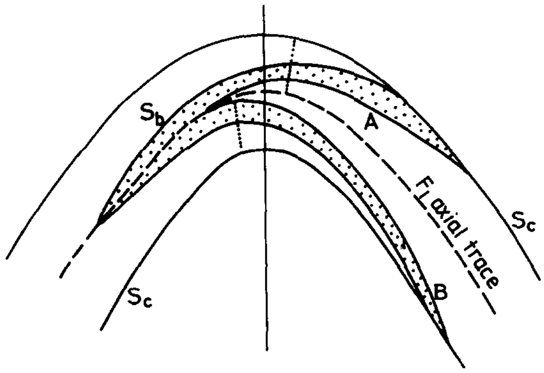

Fig. 11. The hinges and axial surface traces of the F_2 folds on S_b show an offset. The axial traces are not parallel.

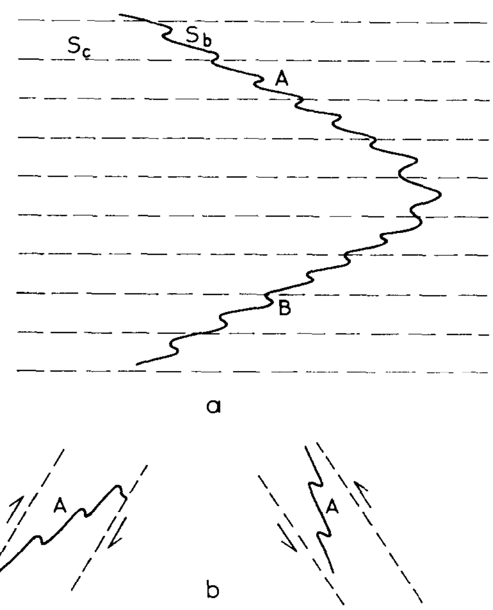

Fig. 13. (a) Z and S folds on the two limbs A and B of a larger F_1 fold. The dashed lines are traces of an axial planar cleavage (S_c). (b) Two domains of the structure on the left and the right limbs of F_2. The arrows indicate the sense of simple shear displacements on S_c. The original shapes of the Z folds of limb A are retained in this figure. This shape will be modified by flexural slip as in Fig. 10 (b) & (c).

There may be smaller asymmetric S- and Z-folds congruous with the larger F_1 (Fig. 13a). During flexural flow folding on the slip surfaces, the shapes of these folds are considerably modified. During the development of an F_2 antiform on S_c, the simple shear is dextral on the left limb and sinistral on the right limb. A layer segment steeper than S_c and dipping in the same direction is extended and thinned on both limbs of the fold on S_c. Similarly, a layer segment S_b dipping at a smaller angle than S_c is shortened and thickened. The longer limbs of the Z-folds on the left side of F_2 (Fig. 13b) are therefore shortened and thickened (Fig. 10a & b). Consequently, the initial asymmetry of the folds changes in the sense that the ratio of short and long limbs comes closer to unity and there is also an increase in angle between the axial plane and the enveloping surface. On the other hand, the asymmetry of the folds is accentuated by the thickness contrast between the two limbs, because up to a certain stage of their development, the shorter limbs of the initial Z-folds are greatly thinned with respect to the longer limbs (Fig. 10a & b). When the same set of Z-folds are rotated on the right hand side of an antiformal F_2 (Fig. 13b), the folds continuously become more asymmetric in the sense that the initial longer limbs of the folds are further lengthened and the initial shorter limbs are shortened (Fig. 10c). The angle between the enveloping surface and the axial plane also decreases to a considerable extent. The initial asymmetry of the S-folds on limb B of F_1 is modified in an opposite manner. The initial shape and asymmetry of the smaller folds is least modified at the hinge of the F_2 fold on cleavage, although the axial surfaces of the smaller folds become curved. Evidently, the morphology of the folds would deviate further from that of buckling folds if there are three generations of coaxial folds, with flexural flow folding taking place on the axial plane cleavages of the second generation folds (Fig. 10 d–f).

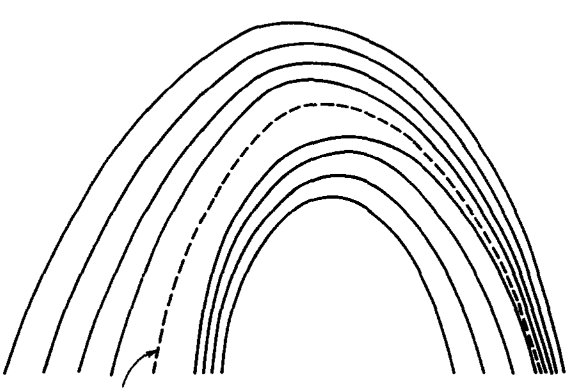

Fig. 12. On any one limb of the F_2 fold the layer-thickness shows different patterns of variation on either side of the F_1 axial trace. Where the F_1 fold closures are unexposed, the F_1 axial trace may be located from such patterns of thickness variation.

It has been assumed in the foregoing analysis that the folds on S_c and S_b are coaxial. If the axis of the second generation flexural flow folds (F_{2c}) on the axial planar cleavage of a first generation fold (F_1) is at an angle to the F_1 axis, the axes of the second generation folds on the bedding (F_{2b}) will be differently oriented on the two limbs of F_1. Neither of them will be parallel to the axis of F_{2c}. Since the cleavage is axial plannar to F_1, the bedding–cleavage intersection lineation is parallel to the F_1 axis. On the folded cleavage surfaces, the traces of bedding will maintain a constant angle with the F_{2c} axis (Fig. 14); the lineation will be straightened out when the fold on the cleavage is unrolled. On the other hand, on any cylindrical segment of a F_{2b} fold the bedding–cleavage intersection lineation will not maintain a constant angle with the axis of F_{2b} (Fig. 14). When the fold is unrolled the lineation will appear curved.

SUMMARY AND CONCLUSIONS

The simple shear (γ) at any point of a flexural flow fold on S_c is equal to the dip angle (θ) at that point, i.e. the

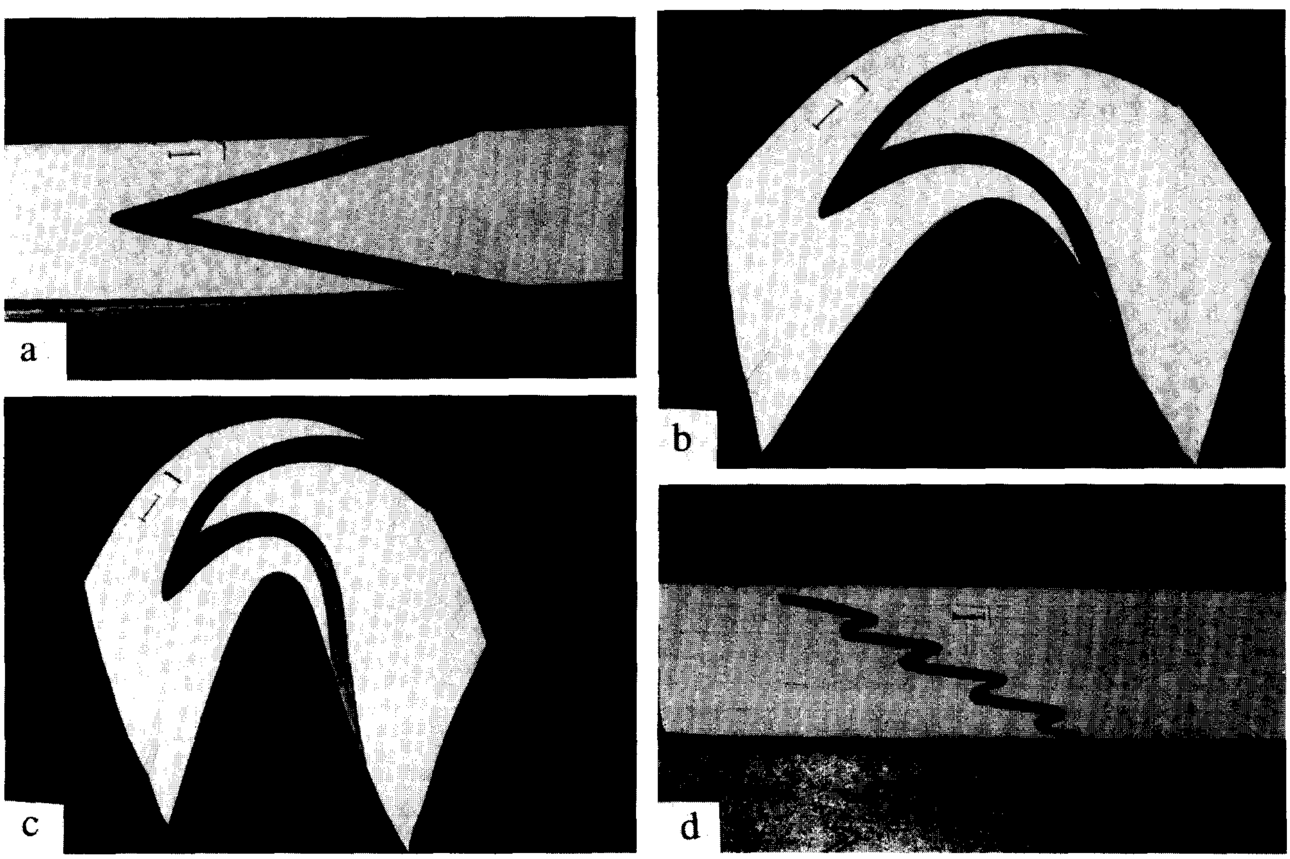

Fig. 9. (a) Paper stack model with profile of F_1 fold drawn on the vertical edge. The traces of the sheets are parallel to the axial surface trace of F_1. (b) and (c) Two stages of flexural slip folding of the paper stack shown in (a). (d) Paper stack model with the profile of asymmetric Z-folds drawn on the edge.

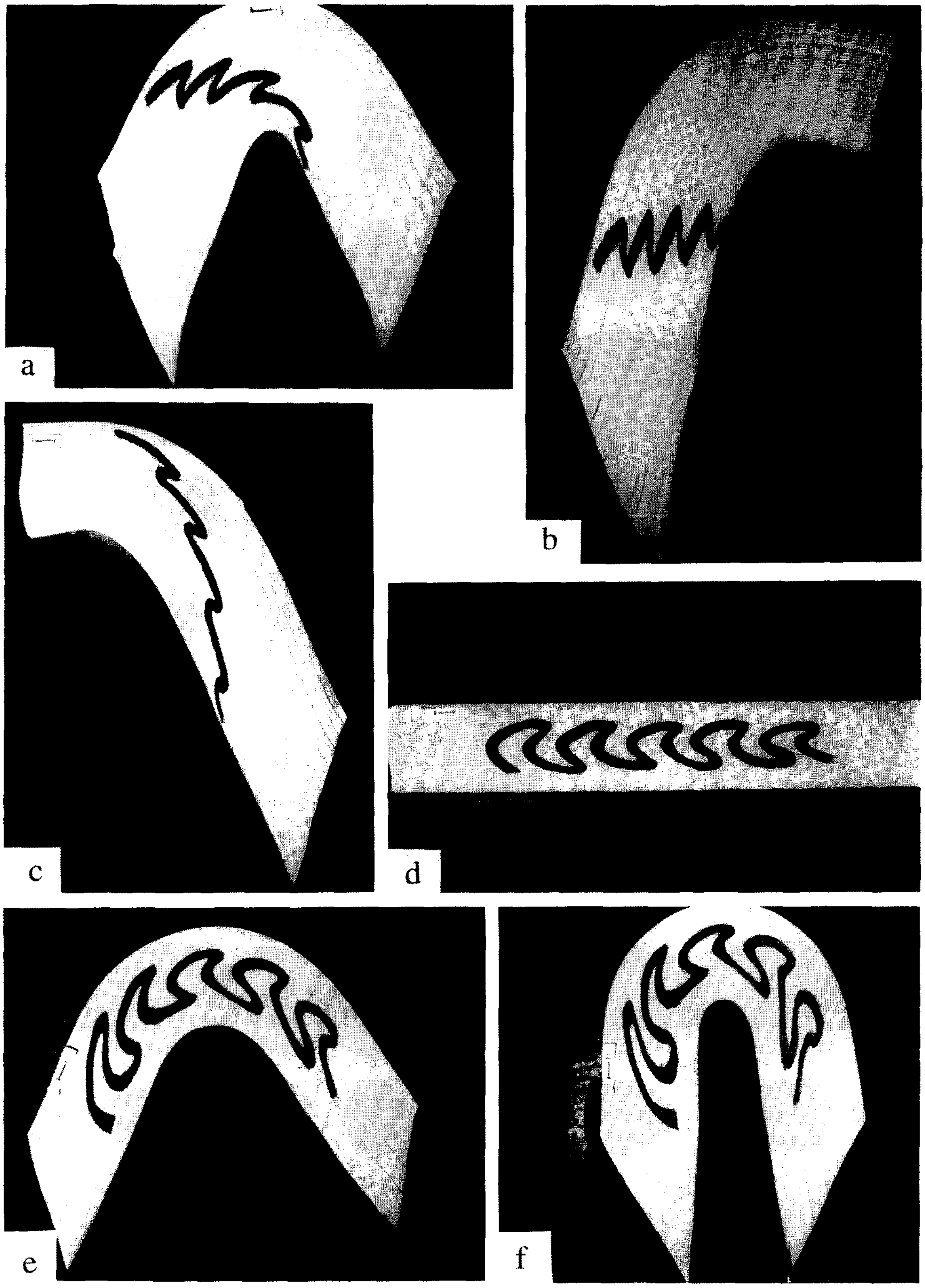

Fig. 10. (a) Deformation of Z-folds shown in Fig. 9(d). Note the different manner in which the initial asymmetry of the folds has changed on the two limbs of the flexural slip fold. (b) Flexural slip folding of Z-folds shown in Fig. 9(d). The sense of simple shear is the same as on the left limb of an antiformal fold. (c) Same as in (b) but with sense of simple shear as on right limb of an antiformal fold. (d) Undeformed paper stack with a two-dimensional type 3 interference pattern drawn on the edge, with the traces of the paper sheets parallel to axial traces of F_2 folds drawn on the edge. (e) and (f) Two stages of deformation of the hook-shaped pattern of (d) by flexural slip folding of the paper stack.

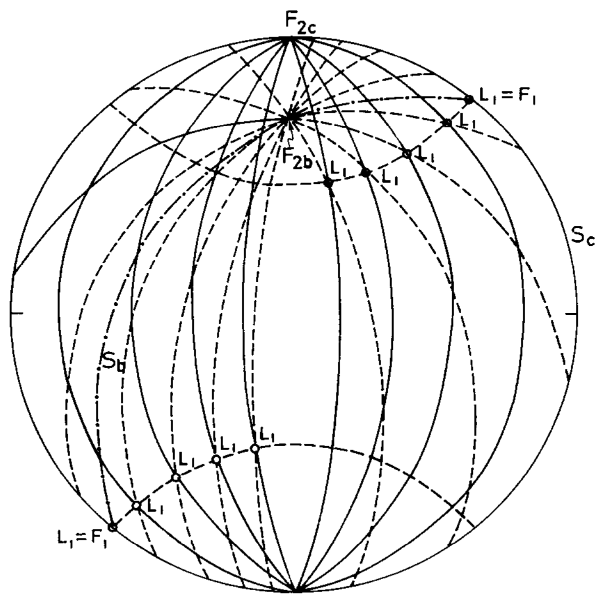

Fig. 14. Lower hemisphere stereographic projection showing initial horizontal orientation of S_c (solid line) and an intersecting layer S_b (dot-and-dash line) with an intersection lineation L_1 parallel to the F_1 axis. The axes of the second generation folds on S_c and S_b, F_{2c} and F_{2b}, are not parallel. Continuous great circles are limbs of F_{2c}. Dashed great circles are limbs of F_{2b}. L_1 is externally rotated around F_{2c}. However, the angle between F_{2b} and the rotated L_1 does not remain constant.

angle between S_c at that point and at the hinge point of the fold. This important relationship, valid for folds of any shape in which the dip angle continuously increases from the hinge to the inflection point, enables us to predict the variation in orthogonal thickness of an oblique passively behaving layer folded in response to the flexural flow on the slip surfaces. Coaxial refolding of such layers produces an uncommon geometry, with the orthogonal thickness of the later folds continuously increasing or continuously decreasing from one limb to the other over the fold hinge and with no stationary value at any point. Although the thickness variation of the folds does not conform to any of the standard classes, their converging pattern of dip isogon is similar to that of the parallel fold on the slip surfaces. The refolded smaller folds on the passively behaving layers also show a complex pattern of thickness variation and a strong modification of their initial asymmetry. A comparison of the thickness variation pattern of naturally occurring superposed folds with that of the theoretically derived pattern will enable us to identify flexural flow folds.

Folding of penetrative cleavage surfaces of slates and schists is fairly common. Depending on whether or not it behaves in a passive manner, a layer at an angle to the cleavage may or may not show the pattern of thickness variation in accordance with the model described above. Moreover, the folding of closely spaced well-developed cleavage surfaces may not conform with the idealised model of flexural slip. The nature of the deviation of the pattern from that of the theoretical model may then give us valuable information about the mechanism of folding for the folds on both the layering and the cleavage. This problem is, however, much more complex, and is outside the scope of this paper. If a set of layers (S_b) oblique to the cleavage planes (S_c) does not behave in a passive manner, the folding of each of S_b and S_c may be influenced by that of the other. The folding of the layers will not only be influenced by the mechanical property of the layers but also by the mechanical property of the cleavage. Similarly, the simple shear displacements on the cleavage surfaces may be modified by the active folding of the intersecting layers.

Finally, the theoretical model considered in this paper assumes a uniform thickness of the F_1 limbs before the folding of their axial planar cleavage. If the initial thickness was non-uniform, the thickness variation of the layers will have a more complex pattern over the F_2 folds. However, since the magnitude of simple shear (γ) is known at every point of the fold, the initial thickness t^* and the initial angle ϕ can be determined for each value of θ, so that the initial profile shape of the F_1 fold (not necessarily with straight limbs of uniform thickness) can be reconstructed.

Acknowledgements—I am grateful to Lilian Skjernaa and Richard Lisle for critically reviewing the manuscript and for suggesting improvements.

REFERENCES

Ghosh, S. K. 1995. Side-stepping of axial surface traces in superposed folding. Special volume on Progressive and Superposed Deformations. *Proc. Indian Academy of Sci., Earth and Planetary Sciences* **104**, 373–383.

Ghosh, S. K. & Ramberg, H. 1968. Buckling experiments on intersecting fold patterns. *Tectonophysics* **5**, 89–105.

Ghosh, S. K., Mandal, N., Khan, D. & Deb, S. 1992. Modes of superposed buckling in single layers controlled by initial tightness of early folds. *J. Struct. Geol.* **14**, 381–394.

Ghosh, S. K., Mandal, N., Sengupta, S., Deb, S. K. & Khan, D. 1993. Superposed buckling in multilayers. *J. Struct. Geol.* **15**, 95–111.

Gray, D. R. & Durney, D. W. 1979. Investigations on the mechanical significance of crenulation cleavage. *Tectonophysics* **58**, 35–79.

Hudleston, P. J. 1973. Fold morphology and some geometrical implications of theories of fold development. *Tectonophysics* **16**, 1–46.

O'Driscoll, E. S. 1962. Experimental patterns in superposed similar folding. *J. Soc. Petrol. Alberta* **10**, 145–167.

Ramsay, J. G. 1967. *Folding and Fracturing of Rocks*. McGraw-Hill, New York.

Ramsay, J. G. and Huber, M. I. 1987. *The Techniques of Modern Structural Geology 2.*, Folds and fractures. Academic Press, London.

Skjernaa, L. 1975. Experiments on superimposed buckle folding. *Tectonophysics* **27**, 255–270.

Thiessen, R. 1986. Two-dimensional refold interference patterns. *J. Struct. Geol.* **8**, 563–573.

Thiessen, R. & Means, W. D. 1980. Classification of fold interference patterns: a re-examination. *J. Struct. Geol* **2**, 311–316.